Article:
Yang, X., Ingham, D., Ma, L. et al. (2018) Prediction of particle sticking efficiency for fly ash deposition at high temperatures. Proceedings of the Combustion Institute, 37 (3). pp. 2995-3003. ISSN: 1540-7489

https://doi.org/10.1016/j.proci.2018.06.038

Available online at www.sciencedirect.com

ScienceDirect

Proceedings of the Combustion Institute 000 (2018) 1–9

Proceedings of the Combustion Institute

www.elsevier.com/locate/proci

Prediction of particle sticking efficiency for fly ash deposition at high temperatures

Xin Yang [a], Derek Ingham [a], Lin Ma [a,*], Maurizio Troiano [b], Mohamed Pourkashanian [a]

[a] *Energy 2050, Department of Mechanical Engineering, University of Sheffield, Sheffield S10 2TN, UK*
[b] *Dipartimento di Ingegneria Chimica, dei Materiali e della Produzione Industriale, Università degli Studi di Napoli Federico II, Piazzale Vincenzo Tecchio 80, 80125 Napoli, Italy*

Received 28 November 2017; accepted 3 June 2018
Available online xxx

Abstract

The tendency of ash particles to stick under high temperatures is dictated by the ash chemistry, particle physical properties, deposit surface properties and furnace operation conditions. A model has been developed in order to predict the particle sticking efficiency for fly ash deposition at high temperatures. The model incorporates the particle properties relevant to the ash chemistry, particle kinetic energy and furnace operation conditions and takes into consideration the partial sticking behaviour and the deposit layer. To test the model, the sticking behaviours of synthetic ash in a drop tube furnace are evaluated and the slagging formation from coal combustion in a down-fired furnace is modelled. Compared with the measurements, the proposed model presents reasonable prediction performance on the particle sticking behaviour and the ash deposition formation. Through a sensitivity analysis, furnace operation conditions (velocity and temperature), contact angle and particle size have been found to be the significant factors in controlling the sticking behaviours for the synthetic ash particles. The ash chemistry and furnace temperature dictate the wetting potential of the ash particles and the melting ability of the deposit surface; particle size and density not only control the particle kinetic energy, but also affect the particle temperature. The furnace velocity condition has been identified as being able to influence the selective deposition behaviour, where the maximum deposition efficiency moves to smaller particles when increasing the gas velocity. In addition, the thermophoresis effect on the arrival rate of the particles reduces with increasing the gas velocity. Further, increasing the melting degree of the deposit layer could greatly enhance the predicted deposition formation, in particular for the high furnace velocity condition.

Keywords: Ash deposition; Particle sticking; Slagging; Furnace operation condition; CFD

* Corresponding author.
E-mail address: lin.ma@sheffield.ac.uk (L. Ma).

https://doi.org/10.1016/j.proci.2018.06.038

1. Introduction

Prediction of ash deposition formation is of great importance in the efficient utilisation of various solid fuels and the development of combustion technologies [1–4]. Predicting the particle sticking efficiency is a critical step in modelling the ash deposition formation, which is dictated by the ash chemistry, particle properties, deposit surface properties, and furnace operation conditions. Ash chemistry dictates the melting potential and the rheology of ash particles, which controls how the molten/partially molten ash particles behave when impacting on the heat exchanger surfaces. In addition, ash chemistry is important in dictating the degree of sintering of the deposits, which is relevant to the removal of deposits [5]. Deposit surface properties are important in controlling the spreading behaviour and the energy dissipation of the ash particles impacting on the surfaces. Further, the surfaces could gradually become sticky due to the formation of the liquid phase on the deposit layer [6,7]. High furnace temperature promotes the melting of ash particles and the formation of the sticky deposit layer. The decrease in the furnace velocity condition under oxy-coal combustion condition in a small scale furnace could increase the deposit accumulation compared to the air-fired combustion condition [8]. Without enough air transported into the combustion chamber incurs a delay in the combustion and this can aggravate the pyrite-induced slagging formation in the furnace [9].

Many researches have been performed to predict the particle stickiness in order to calculate the ash deposition rate. Walsh et al. [6] proposed the particle sticking model, where the stickiness is inversely proportional to ash viscosity based on the assumption that the sticking efficiency increases with an increase in the contact area between the ash droplets and the deposit surface. The other widely used model is based on the melting behaviour proposed by Tran et al. [10], which assumes that only when ash particles or deposited surface has a certain liquid phase content then it is possible for particles to be sticky. Both two particle sticking models attempt to take into consideration the ash chemistry and furnace temperature. However, there exist large discrepancies in the criterion values due to the negligence of the particle kinetic energy in these two models [11–13]. On the other hand, Mao et al. [14] developed a semi-empirical droplet sticking/rebounding model through an energy conservation analysis of the spread and rebound of liquid droplets. The model takes into consideration the main parameters (contact angle, viscosity, surface tension, droplet size and density) in controlling the sticking behaviours of liquid droplets. Mueller et al. [15] predicted the rebounding behaviour of large particles for the ash deposition formation in an entrained flow reactor by employing the energy conservation based model [14,16]. Ni et al. [17] evaluated the sticking potential of slag droplets through using the similar particle sticking/rebounding model. It was found that under high velocity conditions (3-20 m/s), the sticking potentials of slag droplets increase with increasing the particle velocity and particle size, which is inconsistent with the predicted sticking behaviour of slag droplets by Balakrishnan et al. [18], where slag droplets have higher sticking potential with the lower particle size and impact velocity. Recently, Kleinhans et al. [19] explained the deposition phenomenon of the small aluminum silicate particles and the large iron-rich particles through employing a similar energy based particle sticking/rebounding model. The prediction performance of the energy conservation based model is dependent on the prediction of the maximum spread factor during the impaction process, which was derived from the spreading of water droplets with particle Reynolds number much higher than that for the ash droplets [14,16]. In addition, the partial sticking phenomenon has been found in the experimental investigations of sticking behaviours of the droplets which have small excess energy after impaction [20–22], which is neglected in the energy conservation based particle sticking models [14,17–19]. It is clear that the current energy conservation based particle sticking/rebounding model still needs further development.

This paper aims to develop an improved particle sticking model based on the energy conservation analysis during the particle impaction processes for ash droplets. The proposed model considers the ash chemistry, particle physical properties, deposit surface properties and furnace operation conditions. In addition, a sensitivity analysis of the major parameters in controlling the particle sticking efficiency has been investigated using the new model developed. Two different previous experimental results on particle sticking behaviours have been used to validate the proposed particle sticking model, including (i) the soda-lime glass particles sticking experiments by Srinivasachar et al. [23], and (ii) the ash deposition experiments during coal combustion in a down-fired furnace by Beckmann et al. [13].

2. Particle sticking model

Slagging of ash droplets on heat exchanger tubes can be described by the spread and sticking of droplets impacting on a target surface [14,24], as shown in Fig. 1. For normal impacts, at stage 1, just before impaction, ash droplets possess kinetic energy, E_{KE1}, and surface energy, E_{SE1}. During impaction, ash droplets spread on the tube surface due to the inertial and viscous forces. The kinetic energy is transferred to the surface energy and partially dissipated in overcom-

Please cite this article as: X. Yang et al., Prediction of particle sticking efficiency for fly ash deposition at high temperatures, Proceedings of the Combustion Institute (2018), https://doi.org/10.1016/j.proci.2018.06.038

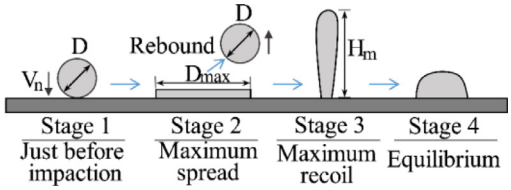

Fig. 1. Sticking/rebounding process after the impaction of ash droplets on the heat exchanger tube surface (modified from [14,24]).

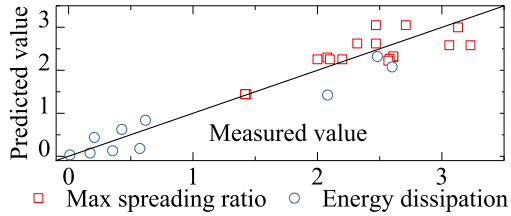

Fig. 2. Comparison of the predicted and measured value for the maximum spreading ratio ($R^2 = 0.67$) and energy dissipation ($R^2 = 0.92$) by using the derived correlations.

ing the viscous force due to the deformation. At stage 2, on reaching the maximum spread diameter, the flattened ash droplets have no kinetic energy and possess the maximum surface energy, E_{SE2}. After that, the splats gradually recoil upwards. At stage 3, on reaching the maximum recoil, the flattened ash droplets have no kinetic energy, and possess surface energy, E_{SE3}, and potential energy, E_{PE3}. At stage 4, the excess energy is dissipated and the droplets reach equilibrium and stick to the heat exchanger tube surfaces. It is assumed that, if ash droplets have enough energy to provide the ash droplets to detach from the surfaces with the original spherical shape (surface energy equal to E_{SE1}), the rebound of the ash droplets upon impacting on the tube surfaces occurs [14]. At the rebound stage, the potential energy is neglected due to its small value compared to surface energy. Therefore, the rebound criterion can be formulated as follows:

$$\begin{aligned} E^* &= \frac{1}{E_{SE1}}[(E_{SE3} + E_{PE3}) - E_{SE1}] \\ &= \frac{1}{E_{SE1}}[(E_{SE2} - E_{Diss2\to3}) - E_{SE1}] \end{aligned} \quad (1)$$

where, E^* is the excess energy normalized by the surface energy (E_{SE1}) in stage 1, and $E_{Diss2\to3}$ is the energy dissipated between stages 2 and 3. E_{SE1} and E_{SE2} can be expressed as:

$$E_{SE1} = \pi D_0^2 \gamma_{LV} \quad (2)$$

$$\begin{aligned} E_{SE2} &= E_{SE\_LV} + E_{SE\_SL} - E_{SE_{SV}} \\ &= \pi D_0^2 \gamma_{LV}\left[\frac{1}{4}d_m^2(1 - cos\theta) + \frac{2}{3d_m}\right] \end{aligned} \quad (3)$$

where, D_0 is the particle size of the ash droplets; E_{SE_LV}, E_{SE_SL} and E_{SE_SV} are the liquid-vapour surface energy, the solid-liquid surface energy, and the solid-vapour surface energy, respectively; γ_{LV} is the liquid-vapour surface tension; d_m is the maximum spread ratio, defined as the ratio of the maximum spread diameter to the original droplet size, D_0; θ is the contact angle. The contact angle could decrease with increasing the furnace temperature and the melting potential of the ash particles (relevant to ash chemistry) [19,25]. In addition, the apparent contact angle should be used when the surface roughness of the heat exchanger tube is taken into account in the spread and impaction of the ash droplets [14,20]. The maximum spread ratio of the ash droplets is assumed to be dependent on the particle Weber number under high temperatures and the particle Reynold number is not directly considered. Due to the limitation in obtaining the spreading data of ash droplets, the experimental spreading data of the sucrose and ink droplets from [14,26], which have much lower particle Reynolds number (approximately 30–1000) than water droplets (higher than 4000) [14,26], is employed to obtain the empirical correlation of the maximum spread ratio using the linear regression analysis (as shown in Fig. 2):

$$d_m = 1 + 0.259 * We^{0.317} \quad (4)$$

where, $We = (\rho_p {U_p}^2 D_0)/\gamma_{LV}$ is the particle Weber number, ρ_p is the density of the ash droplets; U_p is the normal component of the impact velocity of the ash droplets. Based on the assumption that the energy dissipation ($E_{Diss2\to3}$) is a function of the maximum spread ratio and the contact angle [14], $E_{Diss2\to3}$ can be obtained based on the experimental data [14,20,23] using partial least square regression (as shown in Fig. 2):

$$E_{Diss2\to3} = \pi D_0^2 \gamma_{LV}\left[0.00536 * {d_m}^{4.70} * (1 - cos\theta)^{0.591}\right] \quad (5)$$

Substituting Eqs. (2), (3) and (5) into Eq. (1), the excess energy ratio (E^*) can be expressed as:

$$\begin{aligned} E^* = &\frac{1}{4}d_m^2(1 - cos\theta) + \frac{2}{3d_m} \\ &-0.00536 * {d_m}^{4.70} * (1 - cos\theta)^{0.591} - 1 \end{aligned} \quad (6)$$

For $E^* \le 0$, the sticking efficiency, E_{stick}, equals to unity. By considering the partial sticking/rebound phenomenon of the droplets with the excess energy slightly larger than zero, the sticking efficiency is assumed to be a function of the excess energy ratio, E^*. It is assumed that the sticking efficiency of droplets is not significant when the droplets lose more than half of the incoming surface energy [27], which represents the sticking

Please cite this article as: X. Yang et al., Prediction of particle sticking efficiency for fly ash deposition at high temperatures, Proceedings of the Combustion Institute (2018), https://doi.org/10.1016/j.proci.2018.06.038

Table 1
Properties of the soda-lime glass particles.

Glass properties, T represents temperature in °C		Ash composition, %	
Contact angle, °	$180/(1+e^{\frac{T-930}{100}})$	SiO_2	72
Surface tension, N/m	$0.66-0.0003*T$	Na_2O	15
Viscosity, Pa s	$10^{(-2.92+\frac{4700.76}{T-218.13})}$	CaO	8
Density, kg/m^3	$2535-0.143*T$	MgO	5

efficiency, E_{stick}, being negligible when the excess energy ratio is larger than 0.5. The sticking efficiency, E_{stick}, can be expressed by an exponential formulation as:

$$E_{stick} = \exp(a * E^*), \text{ if } E^* > 0 \quad (7)$$

where, $a = -9.21$ to satisfy the above assumption that $E_{stick} = 0.01$ (a small value for the exponential formulation) when $E^* = 0.5$. Since the stickiness of the molten/partially molten deposit layer could be attributed to the liquid phase content [28,29], it is assumed that the formation of the deposit layer can reduce the excess energy ratio by a factor related to its melting degree. Therefore, the sticking efficiency, E^*_{stick}, can be further expressed as follows:

$$E^*_{stick} = \exp[-9.21 * E^*(1-f_{melt})], \text{ if } E^* > 0 \quad (8)$$

where, f_{melt} is the liquid phase content (or termed as the melt fraction) of the deposit surface, which is estimated by the deposit composition and temperature through the chemical equilibrium method.

3. Case descriptions

3.1. Case 1: sticking behaviour of synthetic ash particles

Synthetic ash particles (soda-lime glass) with diameters ranging from 53 μm to 74 μm were used to investigate the sticking behaviour under different furnace temperatures (ranging from approximately 890 K to 1225 K). More details of the deposition experiments can be found in the work of Srinivasachar et al. [23]. The properties (ash composition, contact angle, surface tension, viscosity, and density) of the used soda-lime-glass particles are shown in Table 1 [19,23]. Deposition experimental results show that: (i) glass particles start to stick on the probe at 1075 K and the sticking efficiency sharply increase to unity at a temperature of 1225 K when the particle velocity is 4 m/s and (ii) ash deposition occurs at lower temperature when reducing the particle kinetic energy.

3.2. Case 2: slagging formation from coal combustion

The South African Middelburg coal was used to investigate the ash deposition behaviour in a drop tube furnace. More details of the deposition experiments can be found in the work of Beckmann et al. [13]. The fly ash deposition results at the lower location in the furnace, where the char burnout is approximately 99.4% and the effect of the unburned char on the ash deposition is assumed to be negligible, are modelled in this study. The fly ash properties (ash composition, particle size, and particle loading) and the furnace conditions are from the work of Beckmann et al. [13], and other properties (particle density, particle specific capacity, and surface tension) are estimated based on the ash composition, as shown in Table 2 [17,30–32]. Since there is no experimental data on the contact angle, a value of 135° is used in the current study, which produces a good correlation with the measurements of the deposition rate. An uncertainty study of the contact angle ranging from 120° to 160° indicates that the value of the deposition rate ranges from 0.59 to 1.54 g/h for the uncooled probe and 0.66 to 2.03 g/h for the cooled probe.

CFD modelling is carried out to predict the fly ash deposition behaviour. ANSYS Fluent version 16.1 has been employed to perform the basic calculations, incorporating the user-defined routine DEFINE_DPM_EROSION in order to predict the ash deposition formation [12,33]. Mathematical submodels, such as the Realizable k-ε model with the enhanced wall treatment, Discrete Ordinate model and Discrete Phase Model (DPM), were used for modelling the turbulence, radiation heat transfer and particle trajectories, respectively. Both the gravitational force and the thermophoretic force by Talbot et al. [34] are considered for predicting the particle trajectories. The computational domain is considered to be a 2D geometry (0.3 m*0.6 m) with a deposition tube of outer diameter 22 mm placed in the central region. A fine mesh, which meets the size requirements for predicting the particle impaction behaviour [35], is distributed around the deposition probe. It should be noted that, in the CFD simulations, the particle diameters (ranging from 1 μm to 150 μm) with 50 intervals are used since the difference in the predicted particle arrival rate is approximately 5% compared to the results with 150 intervals. In addition, the "steady state" assumption is used for both the cooled (600 °C) and uncooled probes since this study focuses on the ash deposition formation at the early stage in a small time interval. However, a dynamic model is required for predicting the whole

Please cite this article as: X. Yang et al., Prediction of particle sticking efficiency for fly ash deposition at high temperatures, Proceedings of the Combustion Institute (2018), https://doi.org/10.1016/j.proci.2018.06.038

Table 2
Fly ash properties and furnace conditions used in the CFD simulations.

Fly ash properties, T represents temperature in °C		Ash composition, %	
Size distribution, μm	Rosin-Rammler, D_{mean} (21), spread parameter (0.76)	SiO_2	38.6
Particle loading, kg/h	$1.983^{*}10^{-2}$	Al_2O_3	32.3
Density, kg/m^3	3333	Fe_2O_3	5.8
Specific capacity, J/(kg K)	$975.65 + 0.23 * (T + 273.15) + 0.24/(T + 273.15)^2$	CaO	12.3
Surface tension, N/m	$0.415 + 0.004 * (T - 1400)/100$	MgO	2.0
Viscosity, Pa s	$10^{(-8.07+\frac{14100.72}{T+273.15})}$	TiO_2	1.9
Furnace conditions		Na_2O	0.9
Gas temperature, °C	1125	K_2O	1.1
Gas velocity, m/s	0.357	P_2O_5	2.0
O_2, vol% (dry)	3.68	SO_3	3.1
CO_2, vol% (dry)	15.7		

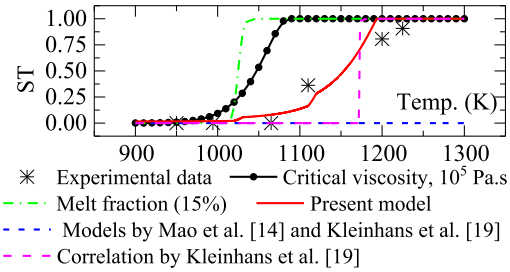

Fig. 3. Comparison of the sticking efficiency (ST) between the sticking models and measurements as a function of temperature. (For more details of the particle sticking models used, please refer to the supplemental material. The same usage of the particle sticking models is applied to Case 2, as shown in Fig. 5).

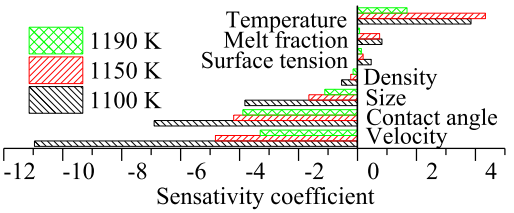

Fig. 4. Sensitivity analysis of the main factors on the sticking efficiency for the soda-lime glass particle (size-63.5 μm and velocity-4 m/s). (For more details of the sensitivity analysis, please refer to the supplemental material.).

ash deposition growth process in order to consider the effects of the deposit surface conditions (surface temperature, deposit shape, etc.) [32,33,36].

4. Results and discussion

4.1. Case 1: evaluation of sticking efficiency for synthetic ash

Figure 3 shows the sticking efficiency as a function of temperature among the different sticking models. Compared to the viscosity based model (criterion value, 10^5 Pa.s [23]), the melt fraction based model (criterion value, 15% [10]), the other energy conservation based particle sticking models proposed by Mao et al. [14] and Kleinhans et al. [19], and the empirical correlation proposed by Kleinhans et al. [19], the predicted sticking efficiency only when using the present model is more consistent with the experimental data, where the sticking efficiency rapidly increases from zero to unity in the temperature range from 1050 K to 1200 K. Figure 4 shows the sensitivity analysis of the main factors on the sticking behaviour of the soda-lime glass particles while varying the temperature. First, the factors (including particle velocity, contact angle, size, and density) have negative sensitivity coefficients, which represent that on increasing the values of these factors reduces the sticking propensities, while the temperature, surface tension and melt fraction have an opposite trend. These predicted results are in accordance with the previous experimental observations: (i) soda-lime glass particles with less kinetic energy being easier to stick on the probe [23], (ii) droplets impaction on the substrates with a higher contact angle being less sticky [14,37,38], and (iii) ash slag with higher surface tension having the larger adhesion of work and bond strength [39]. Second, the velocity, temperature, contact angle and particle size have the higher sensitivity coefficient to the other factors investigated, which is due to the significant role in determining the maximum surface energy and the energy dissipation.

4.2. Case 2: evaluation of deposition rate for coal combustion

Figure 5 shows the slagging rate between the experimental and predicted results by the different particle sticking models. The predicted slagging rates from the present model and the predicted results from Beckmann et al. [13] obtained by using the viscosity based model (criterion value, 25 Pa.s) are close to the measurements. Figure 6 presents the

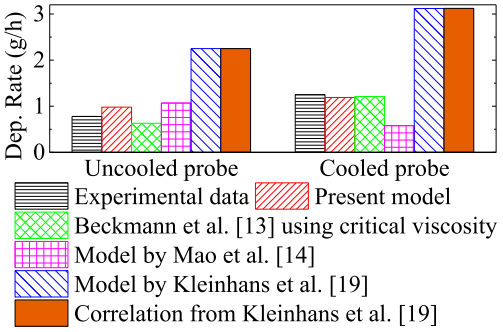

Fig. 5. Comparison of the deposition rates between the sticking models and the measurements.

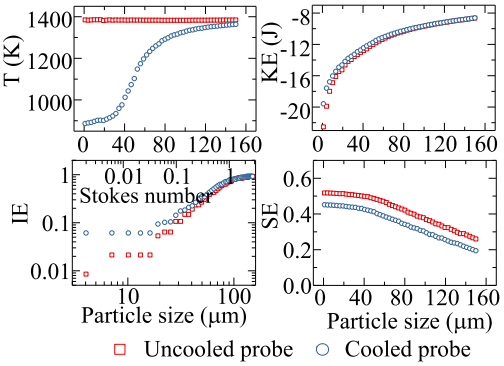

Fig. 6. Predicted deposition behaviours of the fly ash particles: T, KE, IE, and SE are the mass averaged particle temperature, $\log_{10}$ (kinetic energy), impaction efficiency and sticking efficiency, respectively.

detailed deposition behaviours as a function of the particle size through the present model. First, thermophoresis increases the impaction efficiency of the small ash particles on the cooled probe, which results in a higher slagging rate for the cooled probe as observed in both the predicted results and measurements. Second, the predicted particle sticking efficiency is slightly higher (by 0.05–0.10) for the uncooled probe in this study. Third, small particles have a much higher sticking efficiency than the coarse particles and this is because of the lower kinetic energy in the small particles. However, the viscosity based particle sticking model may lead to an opposite relationship between the sticking efficiency and the particle size for the cooled probe as the smaller particles have lower temperature than the larger particles at the cooling stage. In addition, for the uncooled probe, the particle sticking efficiencies when using the viscosity based model could be similar for ash particles with different sizes.

The furnace velocity condition is quite different among the combustors (lab-scale, pilot-scale and utility boiler) although the smaller scale combustors are carefully designed to match the

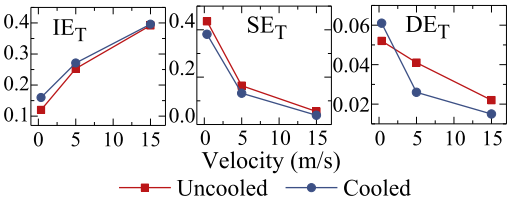

Fig. 7. Predicted deposition behaviours with increasing the gas velocity: IE_T, SE_T, and DE_T represent the overall impaction efficiency, overall sticking efficiency and overall deposition efficiency, respectively.

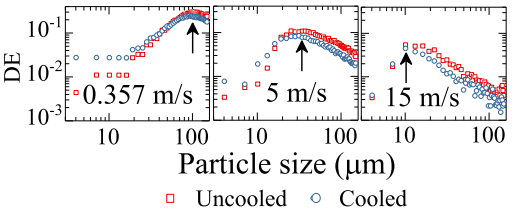

Fig. 8. Predicted deposition efficiency as a function of particle size under different gas velocity conditions.

time-temperature history of the particles within utility boilers [40]. A further analysis is carried out by gradually increasing the gas velocity of the baseline CFD cases with the original gas velocity (0.357 m/s). Figure 7 presents the predicted deposition behaviours of the current fly ash particles at different gas velocity conditions. The overall particle impaction efficiency (for all particles in the projected surface) increases from approximately 10% to 40% and the overall sticking efficiency (for all arrival particles on the probe surface) decreases from approximately 45% to 4% with increasing the gas velocity up to 15 m/s, which results in the decrease in the overall deposition efficiency (defined as the impaction efficiency*sticking efficiency) from approximately 6.1% to 1.5%. In addition, under a higher gas velocity, the deposition efficiency for the uncooled probe could be higher than the cooled probe. This is because the thermophoretic effect on the fly ash deposition behaviour gradually reduces with increasing the gas velocity. The cooling effect from the cooled deposition probe reduces with increasing the gas velocity. Figure 8 shows the deposition efficiency as a function of particle size under different gas velocity conditions. The maximum deposition efficiency gradually changes from the coarse particle size region (100 μm) in the low gas velocity condition to the medium/small particle size region (10–30 μm) in the high gas velocity conditions. This indicates that the selective deposition behaviour is relevant to the gas velocity conditions in combustors. Barroso et al. [41,42] experimentally found that increasing the particle size could increase the ash deposition potential in an entrained flow reactor ($\approx$0.5 m/s) while Raask

Please cite this article as: X. Yang et al., Prediction of particle sticking efficiency for fly ash deposition at high temperatures, Proceedings of the Combustion Institute (2018), https://doi.org/10.1016/j.proci.2018.06.038

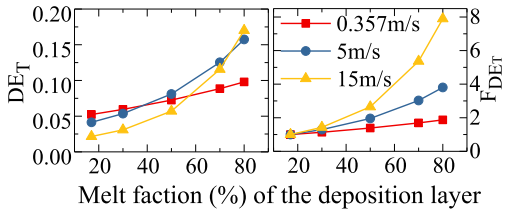

Fig. 9. Predicted overall deposition efficiency as a function of the melt fraction in the deposit layer: the enhancement factor, $F_{DET} = DE_T/DE_{T0}$; DE_{T0} is the overall deposition efficiency for the baseline case.

[39] presented that small particles (around 10 μm) deposit easier than larger particles in utility boilers ($\approx$ 10–25 m/s). Another further analysis is carried out by gradually increasing the melting degree of the deposit layer. Figure 9 shows the effect of increasing the melting degree of the deposit layer on the predicted overall deposition efficiency. Interestingly, the enhancement factor (8 times when using the melt fraction with 80%) for the case with the highest gas velocity is much larger than the other two cases. This indicates again that sticking and deposition behaviour are strictly related to the global and local velocity conditions.

4.3. Remarks on the current particle sticking model

In this paper, an improved particle sticking method is developed based on the energy conservation analysis. Compared with the experimental results in the particle sticking behaviour of the soda lime glass particles and the slagging formation from coal combustion, the proposed model has a good prediction performance. The sensitivity analysis shows the significant role of particle velocity, temperature, contact angle and particle size in determining the particle sticking efficiency of the synthetic ash particles. Further analysis indicates that the selective deposition behaviour is relevant to the gas velocity conditions in the furnaces. In addition, increasing the melting degree of the deposit surface could significantly increase the sticking efficiency and enhance the deposition formation, especially for the large gas velocity conditions. High furnace temperature and tube surface temperature could increase the particle stickiness and promote the formation of the sticky deposit layer, which results in the rapid deposit accumulation. In addition, controlling the gas velocity could alleviate the deposit accumulation on the sticky deposit layer since fewer particles are able to impact on the tubes under a lower velocity. Also, increasing the contact angle between the ash droplets and the tube surface could reduce the ash deposition rate, which is in accordance with the findings by Naganuma et al. [37,38], where the surface coatings are used to increase the contact angle and control the ash deposition formation.

The main assumption of the current sticking model is that the sticking behaviour of fly ash deposition under high temperatures could be described by the spread and sticking of the droplets. However, impacting ash particles may not be completely molten, especially in the superheater region where the flue gas temperature is possibly lower than the ash fusion temperatures. In the proposed model, the presence of the solid phase in the ash particles is indirectly considered by its effect on the particle wetting properties (contact angle and surface tension), which is dependent on the temperature and ash chemistry. This consideration is consistent with the results reported by Song et al. [25] and Kleinhans et al. [19], where it was shown that, with decreasing temperature of ash, the contact angle increases along with the decrease in the melting potential. It should be noted that ash viscosity is not directly considered in the present model. In the work of Bennett and Poulikakos [43], the surface tension is significant to the spread factor even well into the viscous dissipation domain, while the effect of viscous dissipation rapidly disappears in the surface tension domain. This outcome confirms the important role of the contact angle during the spreading of particles. Viscosity contributes to part of the energy dissipation [14], but the energy could not be hugely dissipated by an increase in the viscosity because ash particles are easier to rebound with the decrease in the temperature. In addition, the spreading data of relatively viscous droplets were chosen to develop the current model. Accurate treatment of the viscosity in the prediction of the spreading behaviour and the energy dissipation for coal ash requires the detailed knowledge of the role of viscosity in the spreading behaviour during coal ash droplet impaction on the surface, which needs further investigation. Also, the detailed understanding of the spread and impaction behaviour of ash particles on the deposit layer (porous/sintered layer) needs further study in order to rigorously treat the effect of the deposit layer on the sticking behaviour. In addition, the influence of the residual carbon on the energy dissipation during the particle spreading and impaction should be investigated in order to improve the proposed model. Also, the effect of the impact angle on the energy dissipation requires investigations under a temperature-velocity condition close to real combustors/gasifiers [44], which could be another aspect for improving the proposed model. Note that the bulk ash composition is used for predicting the sticking behaviour of the Case 2 where the coal burned was a low-alkali bituminous. This approximation could be less accurate when the fly ash is highly heterogeneous in ash composition,

Please cite this article as: X. Yang et al., Prediction of particle sticking efficiency for fly ash deposition at high temperatures, Proceedings of the Combustion Institute (2018), https://doi.org/10.1016/j.proci.2018.06.038

especially for fuels with high alkali/pyrite content, which needs the particle based ash composition being used in predicting the particle sticking behaviour.

5. Conclusions

(i) An improved particle sticking model, based on the energy conservation analysis and considering the ash chemistry, particle physical properties, deposit surface properties and furnace operation conditions, has been developed for fly ash deposition at high temperatures. The proposed particle sticking model has been validated by the sticking behaviour of the synthetic ash in a drop tube furnace and the slagging formation from coal combustion in a down-fired furnace through CFD modelling.

(ii) The sensitivity analysis shows that the proposed model is able to consider the main factors in dictating the particle sticking behaviours of the synthetic ash particles. Furnace operation conditions (velocity and temperature), contact angle and particle size are found to be sensitive parameters in determining the particle sticking efficiency.

(iii) Furnace velocity condition affects the selective deposition behaviours of fly ash particles. Increasing the gas velocity can reduce the particle size which has the maximum deposition efficiency. This implies that the coarse fly ash particles are easier to deposit in smaller scale furnaces while the small-medium fly ash particles are easier to deposit in utility boilers. Increasing the melting degree of the deposit layer greatly enhances the deposition formation, especially for large gas velocity conditions.

(iv) Tube surface temperature affects the deposition behaviour via its influence on the particle arrival rate and the formation of a deposit layer. Under the low tube surface temperature and the low gas velocity condition, thermophoresis greatly increases the arrival rate of small particles. Without forming a sticky deposit layer, the deposition rate could be higher for the cooled tube than the uncooled tube. However, if forming an effective deposit layer, the deposition rate is likely to be higher for the uncooled tube than the cooled tube, especially under high velocity conditions.

Acknowledgement

The authors acknowledge the support from the EPSRC grants (EP/M015351/1, Opening New Fuels for UK Generation; EP/K02115X/1, Development and Evaluation of Sustainable Technologies for Flexible Operation of Conventional Power Plants).

Supplementary materials

Supplementary material associated with this article can be found, in the online version, at doi: 10.1016/j.proci.2018.06.038.

References

[1] T.F. Wall, *Proc. Combust. Inst* 31 (1) (2007) 31–47.
[2] Y.Q. Niu, H.Z. Tan, S.E. Hui, *Prog. Energy Combust* 52 (2016) 1–61.
[3] M. Hupa, O. Karlström, E. Vainio, *Proc. Combust. Inst* 36 (1) (2017) 113–134.
[4] P.M. Walsh, A.F. Sarofim, J.M. Beer, *Energy Fuels* 6 (6) (1992) 709–715.
[5] A. Zbogar, F. Frandsen, P.A. Jensen, P. Glarborg, *Prog. Energy Combust.* 35 (1) (2009) 31–56.
[6] P.M. Walsh, A.N. Sayre, D.O. Loehden, L.S. Monroe, J.M. Beér, A.F. Sarofim, *Prog. Energy Combust.* 16 (4) (1990) 327–345.
[7] G.D. Li, S.Q. Li, Q. Huang, Q. Yao, *Fuel* 143 (2015) 430–437.
[8] D.X. Yu, W.J. Morris, R. Erickson, J.O.L. Wendt, A. Fry, C.L. Senior, *Int. J. Greenh. Gas Control* 5 (Supplement 1) (2011) S159–S167.
[9] H.L. Wee, H.W. Wu, D.K. Zhang, D. French, *Proc. Combust. Inst.* 30 (2) (2005) 2981–2989.
[10] H. Tran, X. Mao, D.C.S. Kuhn, R. Backman, M. Hupa, *J. Pulp Paper Sci.* 103 (9) (2002) 29–33.
[11] C. Wieland, B. Kreutzkam, G. Balan, H. Spliethoff, *Appl. Energy* 93 (2012) 184–192.
[12] X. Yang, D. Ingham, L. Ma, A. Williams, M. Pourkashanian, *Fuel* 165 (2016) 41–49.
[13] A.M. Beckmann, M. Mancini, R. Weber, S. Seebold, M. Müller, *Fuel* 167 (2016) 168–179.
[14] T. Mao, D.C.S. Kuhn, H. Tran, *AIChE J.* 43 (9) (1997) 2169–2179.
[15] C. Mueller, M. Selenius, M. Theis, et al., *Proc. Combust. Inst.* 30 (2) (2005) 2991–2998.
[16] M. Pasandideh-Fard, Y.M. Qiao, S. Chandra, J. Mostaghimi, *Phys. Fluids* 8 (3) (1996) 650–659.
[17] J.J. Ni, G.S. Yu, Q.H. Guo, Z.J. Zhou, F.C. Wang, *Energy Fuels* 25 (3) (2011) 1004–1009.
[18] S. Balakrishnan, R. Nagarajan, K. Karthick, *Energy* 81 (2015) 462–470.
[19] U. Kleinhans, C. Wieland, S. Babat, G. Scheffknecht, H. Spliethoff, *Proc. Combust. Inst.* 36 (2) (2017) 2341–2350.
[20] W.K. Hsiao, J.H. Chun, N. Saka, *J. Manuf. Sci. Eng.* 131 (2) (2009) 021010-021001-021010-021018.
[21] M. Troiano, F. Montagnaro, P. Salatino, R. Solimene, *Fuel* 209 (2017) 674–684.
[22] M. Troiano, T. Santagata, F. Montagnaro, P. Salatino, R. Solimene, *Fuel* 202 (Supplement C) (2017) 665–674.
[23] S. Srinivasachar, J.J. Helble, A.A. Boni, *Proc. Combust. Inst.* 23 (1) (1991) 1305–1312.
[24] S. Chandra, C.T. Avedisian, *Proc. R. Soc. A* 432 (1884) 13 (1991).
[25] W.J. Song, Y. Lavallée, F.B. Wadsworth, K.-U. Hess, D.B. Dingwell, *J. Phys. Chem. Lett.* 8 (8) (2017) 1878–1884.

[26] A. Asai, M. Shioya, S. Hirasawa, T. Okazaki, *J. Imaging Sci. Technol.* 37 (1993) 205–207.
[27] S. Singh, D. Tafti, *Int. J. Heat Fluid Flow* 52 (2015) 72–83.
[28] P. Isaac, H. Tran, D. Barham, D. Reeve, *J. Pulp Paper Sci.* 12 (3) (1986) J84–J88.
[29] S.K. Kær, L.A. Rosendahl, L.L. Baxter, *Fuel* 85 (5) (2006) 833–848.
[30] A. Kucuk, A.G. Clare, L. Jones, *Glass Technol.* 40 (5) (1999) 149–153.
[31] K.C. Mills, J.M. Rhine, *Fuel* 68 (7) (1989) 904–910.
[32] F.L. Wang, Y.L. He, Z.X. Tong, S.Z. Tang, *Int. J. Heat Mass Transf.* 104 (2017) 774–786.
[33] X. Yang, D. Ingham, L. Ma, H. Zhou, M. Pourkashanian, *Fuel* 194 (2017) 533–543.
[34] L. Talbot, R.K. Cheng, R.W. Schefer, D.R. Willis, *J. Fluid Mech.* 101 (4) (2006) 737–758.
[35] R. Weber, N. Schaffel-Mancini, M. Mancini, T. Kupka, *Fuel* 108 (2013) 586–596.
[36] M. García Pérez, E. Vakkilainen, T. Hyppänen, *Fuel* 181 (2016) 408–420.
[37] H. Naganuma, N. Ikeda, T. Ito, et al., *Fuel* 106 (2013) 303–309.
[38] H. Naganuma, N. Ikeda, T. Kawai, et al., *Proc. Combust. Inst.* 32 (2) (2009) 2709–2716.
[39] E. Raask, Mineral Impurities in Coal Combustion: Behavior, Problems, and Remedial Measures, Hemisphere Publishing Corporation, New York, USA, 1985, pp. 172–173. 196-197.
[40] X. Yang, D. Ingham, L. Ma, N. Srinivasan, M. Pourkashanian, *Proc. Combust. Inst.* 36 (3) (2017) 3341–3350.
[41] J. Barroso, J. Ballester, L.M. Ferrer, S. Jiménez, *Fuel Process. Technol.* 87 (8) (2006) 737–752.
[42] J. Barroso, J. Ballester, A. Pina, *Fuel Process. Technol.* 88 (9) (2007) 865–876.
[43] T. Bennett, D. Poulikakos, *J. Mater. Sci.* 28 (4) (1993) 963–970.
[44] M. Troiano, R. Solimene, P. Salatino, F. Montagnaro, *Fuel Process. Technol.* 141 (Part 1) (2016) 106–116.

Please cite this article as: X. Yang et al., Prediction of particle sticking efficiency for fly ash deposition at high temperatures, Proceedings of the Combustion Institute (2018), https://doi.org/10.1016/j.proci.2018.06.038